Journal of
Marine Science and Engineering

MDPI

Article

Dynamic Task Allocation for Heterogeneous Multi-Autonomous Underwater Vehicle Collaboration Under Mine Countermeasures Missions

Juan Li [1], Baohua Liu [1], Caiyun Liu [2,*] and Cong Lin [1]

[1] College of Intelligent Systems Science and Engineering, Harbin Engineering University, Harbin 150001, China; lijuan041@hrbeu.edu.cn (J.L.); liubaohua@hrbeu.edu.cn (B.L.); lincong0221@hrbeu.edu.cn (C.L.)
[2] School of Information and Electronic Engineering, Shandong Technology and Business University, Yantai 265600, China
* Correspondence: liucaiyun_hrbeu@163.com

Abstract: The task allocation of autonomous underwater vehicles (AUVs) is a crucial aspect of ocean exploration and mission execution tasks. In a mine countermeasures (MCM) combat scenario, when a new suspicious mission point is detected in the mission area, the heterogeneous multi-AUV system requires reallocation in real time. To address this, a soft time windows consensus-based bundle algorithm with partial reallocation (SWCBBA-PR) is designed. Based on the consensus-based bundle algorithm (CBBA), this algorithm comprehensively considers the underwater communication limitations and introduces the soft time window mechanism and partial reallocation mechanism. Its aim is to solve the partial reallocation problem that arises when new task points appear under the temporal-coupling constraints of complex underwater tasks. The SWCBBA-PR algorithm has been validated through simulation, demonstrating its ability to generate an optimal allocation scheme in the scenario of MCM mission emergence, and it exhibits good convergence performance.

Keywords: autonomous underwater vehicles (AUVs); mine countermeasures (MCM); consensus-based bundle algorithm (CBBA); task allocation

check for updates

Received: 20 January 2025
Revised: 22 February 2025
Accepted: 26 February 2025
Published: 27 February 2025

Citation: Li, J.; Liu, B.; Liu, C.; Lin, C. Dynamic Task Allocation for Heterogeneous Multi-Autonomous Underwater Vehicle Collaboration Under Mine Countermeasures Missions. *J. Mar. Sci. Eng.* **2025**, *13*, 465. https://doi.org/10.3390/jmse13030465

1. Introduction

The current research on MCM mission scenarios focuses on the collaborative task allocation of heterogeneous AUVs. This allocation is based on prior information on suspicious task points. When executing MCM tasks in practice, the multi-AUV system has to start by searching for suspicious task points. After confirming that these points indicate mines, the AUVs then need to neutralize them. Finally, it is necessary to verify if the mine threat has been fully eradicated. That is, different types of AUVs need to execute corresponding subtasks according to the process, which poses complex problems of task temporal coupling. In addition, due to the dynamic nature of the actual combat environment, new tasks may emerge at any time. Therefore, how to achieve rapid and effective task reallocation is also a very important issue.

Centralized task allocation has the advantage of strong global solving capability. However, since data transmission has to go through a single control center, the amount of information to be processed is huge. This makes it difficult to meet real-time requirements and prone to single-point failures during task allocation. Especially in underwater environments, it has poor reliability, maintainability, and anti-interference ability. Distributed task allocation is an approach where intelligent agents within a cluster communicate and negotiate to resolve conflicts based on their respective decision results. Currently, distributed task allocation algorithms basically cover three major types: market-like mechanisms, distributed constraints, and multi-agent decision-making theory. The specific classification is shown in Figure 1. Distributed constraint algorithms can be transformed into the form of a constraint network in which each variable has a separate discrete value range, and there are constraint relationships among them. In the solving process, the goal is to find a certain combination of variables so that the sum of all constraints reaches the maximum or minimum value. The core idea of market-like mechanism algorithms is to use communication and negotiation to solve each problem so as to avoid possible conflict situations. The contract net algorithm includes four steps of "tendering-bidding-winning-confirmation" involving bidders and publishers. The auction algorithm takes tasks as auction items and sells them to the highest bidder through open bidding to complete the allocation.

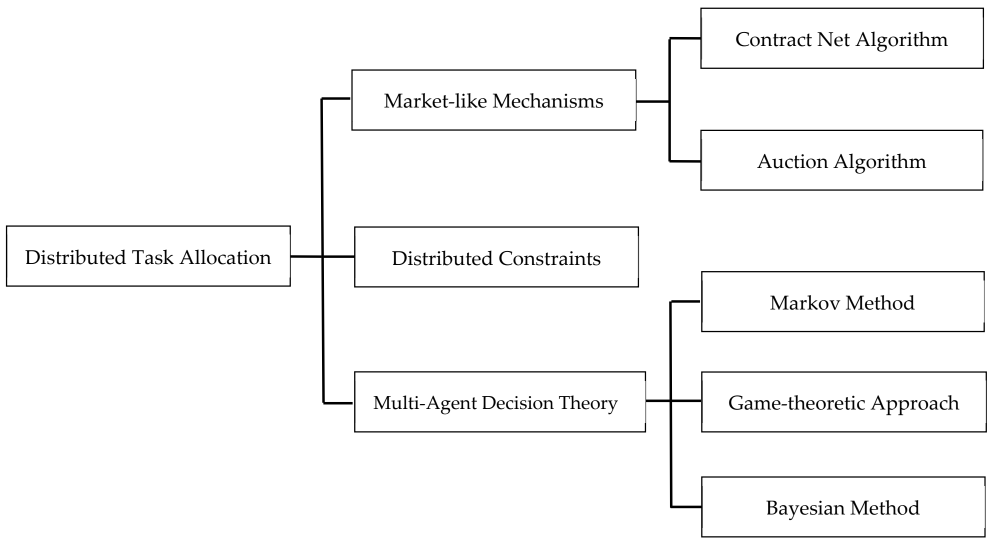

Figure 1. Classification of typical distributed task allocation algorithms.

In reference [1], aiming at the problems of low overall efficiency, unreasonable distribution, and coexistence of multiple bids in the traditional contract network, an improved contract network algorithm was designed by integrating the token ring network and the AUV task load rate standard, which improved the overall effectiveness of the system. In reference [2], for the target search scenario in a complex environment, by combining the improved contract network algorithm (BSE-CNP) with the introduction of a bidder selection mechanism and an improved bid value evaluation mechanism, and the construction of a task reallocation mechanism with the introduction of a virtual decision-maker, the efficiency of the multi-AUV system can be effectively improved, and the global coordination of tasks can be achieved in unforeseen situations. In reference [3], aiming to make up for the deficiencies of the current auction algorithms that do not conform to market laws and ignore the interests of auctioneers, taking the task allocation of heterogeneous multiple AUVs in the situation of limited energy and time-varying ocean currents as the scenario, an improved auction algorithm based on the task reward feedback mechanism was designed. By introducing the robust optimization theory, the adaptability of the multi-AUV system in the complex and changeable marine environment was improved, thus ensuring the utility of the AUV system and reducing the resource consumption of task allocation. In reference [4], a new Consensus-based Adaptive Optimization Auction (CAOA) algorithm was proposed. By introducing an optimization scheme based on the improved particle swarm optimization algorithm, the step size of the price update rule in the distributed auction algorithm was adaptively adjusted, and the key control parameters in the price update function of the bidding algorithm were optimized, reducing the search complexity and thus obtaining better bids. It can obtain higher system gains while greatly reducing the computational amount. In reference [5], after the initial task allocation, a dynamic adjustment strategy was introduced, that is, when to give up or continue the cooperative task. Different from the traditional insistence on impossible tasks, it maximally ensures the benefits of the multi-robot formation, minimizes unnecessary losses and wastes, reduces the task allocation time to the greatest extent, improves the efficiency of task allocation, ensures the safety of task allocation, and increases the stability of the multi-AUV system at the same time.

Currently, distributed task allocation is usually carried out under the assumption of a perfect communication link with infinite bandwidth, and it requires that each member of the system has the same Situation Awareness (SA). In an underwater environment with limited communication, AUVs are unable to interact with information in a timely manner. This causes each AUV to use different information sets for task allocation optimization, thus leading to task allocation conflicts. Therefore, various algorithms evolved from the auction algorithm have been receiving increasing attention, such as the Consensus-Based Bundle Algorithm (CBBA) [6]. This algorithm is realized through iterative processes in two stages: the task bundle stage and the conflict resolution stage. It can reasonably select and arrange the task sequence while taking into account time and other resource constraints, ensuring that the obtained solution achieves at least 50% optimality.

The CBBA algorithm can, to some extent, avoid a large amount of algorithm-related communication. It can also be applied to multi-constraint and dynamic task scenarios. In terms of solving communication problems, reference [7] considers a more realistic cluster that uses asynchronous communication protocols for communication. It proposes the Asynchronous CBBA algorithm (ACBBA) and introduces a replay strategy as a new local conflict resolution rule. These rules do not require access to the global information state. They have the characteristics of consistently processing unordered messages and detecting redundant information, minimizing the communication load while maintaining convergence characteristics. In reference [8], the CBBA based on group consensus (G-CBBA) was proposed. It groups drones based on the task preferences represented by the initial guesses created by the drones. At the same time, nested iterations between local and global planning consensus were introduced. The local stage aims to reach a consensus on the shared task list within the team, while the global stage ensures that the entire cluster reaches a consensus on the entire task set. The proposed two-layer scheme can reduce the propagation of irrelevant bids, maintain the robust convergence of CBBA, and thus improve communication efficiency. In reference [9], an importance ranking model was constructed based on the degree centrality, eigenvector centrality, and mediation centrality of communication UAVs. Then, a set of key nodes was selected from the communication UAVs, and the shortest path principle was used to group and cluster these UAVs. This enables dynamic task allocation among multiple UAVs under limited communication conditions. In Reference [10], the static CBBA was improved into an online algorithm. By integrating the dynamic update of UAV positions and the task convergence flag mechanism, online CBBA (OL-CBBA) was designed to improve the task allocation efficiency of multiple UAVs under weak communication conditions. However, there is currently limited research on non-ideal communication environments such as communication delay, high bit-error rate, and high packet-loss rate. Further exploration is needed on how to improve the adaptability and performance of the CBBA algorithm in non-ideal communication environments while maintaining its basic characteristics and advantages.

Regarding the solution of complex task requirements, in reference [11], considering the critical tasks in the monitoring system, a third phase is introduced. By releasing tasks that exceed the actual capacity, task constraints are met to address the distributed task allocation problem with functional heterogeneity, resource constraints, and critical task allocation guarantee. In reference [12], based on the distance between UAVs and the number and type of payload resources per UAV, the entire UAV cluster is divided into multiple sub-clusters. This simplifies large-scale task allocation into several interrelated small-scale task assignments. The algorithm uses different consensus rules both between and within clusters, ensuring that the drone swarm can obtain conflict-free task allocation solutions in real time. In reference [13], to address the problem of UAV clusters arriving at and executing tasks simultaneously, the CBBA with Time Window (CBGA-TW) was developed. However, this algorithm may generate potential solutions that could lead to deadlocks. In reference [14], a consensus coalition algorithm is proposed. It is used to solve the problem of heterogeneous multi-agent collaborative task allocation under the constraints of load resources and time windows. First, each agent applies the principle of maximizing marginal gain. Meanwhile, it comprehensively considers the time-varying gain of the task and the navigation cost to choose a task combination that suits its characteristics. Second, based on the improved conflict resolution rules, the task conflict problem in task allocation is resolved. In Reference [15], a load distribution matrix was introduced into the CBBA to track the load of robots and task requirements in real time, and a consensus-based payload algorithm (CBPA) was proposed. It aims to solve the problem that when multiple robots execute complex tasks, the decrease in their capabilities due to load consumption makes it difficult for the robot coalition to meet the task requirements in real time. However, the fault tolerance of this algorithm needs to be improved. In reference [16], the Graph Convolutional Network (GCN) is combined with CBBA, and the AI-enhanced CBBA (AI-CBBA) is proposed. This algorithm optimizes the task allocation efficiency of multiple robots by predicting the effectiveness of heuristic extensions through GCN. In reference [17], a non-deadlock sequential extended Consensus-Based Bundle Algorithm is designed. Directed graph depth-first search is introduced to detect and correct deadlock situations in the task plan, aiming to achieve conflict-free and deadlock-free task allocation. At the same time, a sequential layering strategy is adopted to address the temporal constraints of coupled tasks. Moreover, path planning is integrated into task allocation through Dubins curve routes, which enhances the reliability of the task allocation results.

Regarding the solutions to problems in dynamically uncertain task scenarios, in reference [18], when dealing with new online tasks that emerge during the process of solving the task-allocation problem, the CBBA with partial resetting (CBBA-PR) can strike a balance between convergence time and increased cost. It does this by resetting a part of the previously allocated tasks in each round of task bidding. This approach further reduces the communication burden and running time. In reference [19], building on the research in reference [14], the issues arising from new tasks are taken into account. The CBBA with no resetting (NR-CBBA), the CBBA with full resetting (FR-CBBA), and the CBBA with partial resetting (PR-CBBA) are improved. When unknown new tasks appear in the task area, NR-CBBA adds these new tasks after the previously obtained task-allocation plan. FR-CBBA completely abandons the previously obtained task-allocation plan and re-assigns the task sequence upon the addition of new tasks. PR-CBBA re-assigns tasks with the lowest gain released by each agent. All these algorithms can promptly respond to sudden new-task situations. However, the above reallocation algorithms do not fully utilize the original task allocation results and cannot guarantee optimal task reallocation performance in different unexpected situations.

Currently, the improvements based on the CBBA algorithm mostly focus on UAVs, and there is a lack of research on handling complex task coupling constraints and real-time task reallocation in non-ideal communication environments. Due to the communication limitations in the underwater environment, the task allocation of AUV swarms is more particular and challenging. Although many efficient and intelligent task allocation models and algorithms have been proposed and implemented in previous studies, there are still many potential problems that need further exploration; in particular, after considering constraints such as underwater communication, ocean currents, and dynamic targets, the task allocation problem gradually becomes more complex. When designing task allocation algorithms for AUV swarms, the following aspects of problems are generally considered comprehensively:

(1) Real-time issue: The coordinated execution of tasks among multiple AUVs usually requires timely and reliable communication for coordination, which helps ensure the smooth execution of tasks. Since accidents may occur during task implementation, task reallocation is often required. Therefore, how to reallocate tasks in a timely and effective manner to ensure task completion efficiency has become a problem that cannot be ignored. Currently, most of the research focuses on pre-arranged task allocation schemes before task execution; that is, pre-generated schemes. Given the real-time changes in the environment and the real-time updates of task completion status, real-time task reallocation will become an indispensable condition for the intelligent operation of AUVs.

(2) Computational complexity issue: With the increase in the number of AUVs in a multi-AUV system, some of the currently studied task allocation algorithms face the challenge of large computational complexity. For example, the process of task allocation using the auction algorithm involves a single auctioneer and multiple bidders, and the number of bidders is determined according to the algorithm process. The increase in the number of bidders has a direct impact on the system gain and the quality of the task allocation scheme. As the number of bidders increases, the design of the task allocation scheme will become better and the overall coordinated gain will increase, but the computational amount and complexity of the auctioneer will also increase accordingly. Therefore, effectively reducing the computational amount is crucial to the efficiency of the task allocation algorithm and the system's performance.

(3) Communication issue: Communication plays a vital role in the collaborative work of a multi-AUV system. However, most of the current task allocation algorithms are troubled by excessive communication overhead. Excessive communication overhead will directly lead to communication delays, which in turn affect real-time performance and task synchronization, thus reducing the task completion rate. At the same time, an increase in communication volume may cause packet loss or bit errors, affecting the completion of the overall task. Therefore, under limited communication conditions, how to reduce communication overhead and effectively complete task allocation will be a challenging problem.

(4) Heterogeneity issue: The composition of a multi-AUV system is flexible and changeable. Even if the AUVs are homogeneous, there will be certain differences due to the installation of different types of sensors, different communication protocols or communication methods, etc. Meanwhile, even AUVs of the same type cannot maintain the same situation as other members of the system when executing tasks. In this case, the methods applicable to a certain system may not be successfully transferred to other multi-AUV systems. Solving the heterogeneity problem brought about by heterogeneous AUVs is also a major challenge in the task allocation of multi-AUV systems.

In response to the above problems, this paper makes improvements based on the CBBA algorithm and proposes the SWCBBA-PR algorithm. The architecture diagram of the algorithm is shown in Figure 2, and its main contributions are as follows:

(1) Considering the issue of underwater communication limitations, when the trusted communication topology changes, each AUV whose trusted communication status changes is reassigned to ensure effective task allocation.
(2) The time-coupling problem of various subtasks when heterogeneous AUVs execute MCM missions is solved by introducing soft time window constraints.
(3) When new suspicious task points emerge, the relationship between the new tasks and the original task allocation plan can be comprehensively considered, and partial reallocation can be carried out based on the original plan. This improves the efficiency and speed of task reallocation.

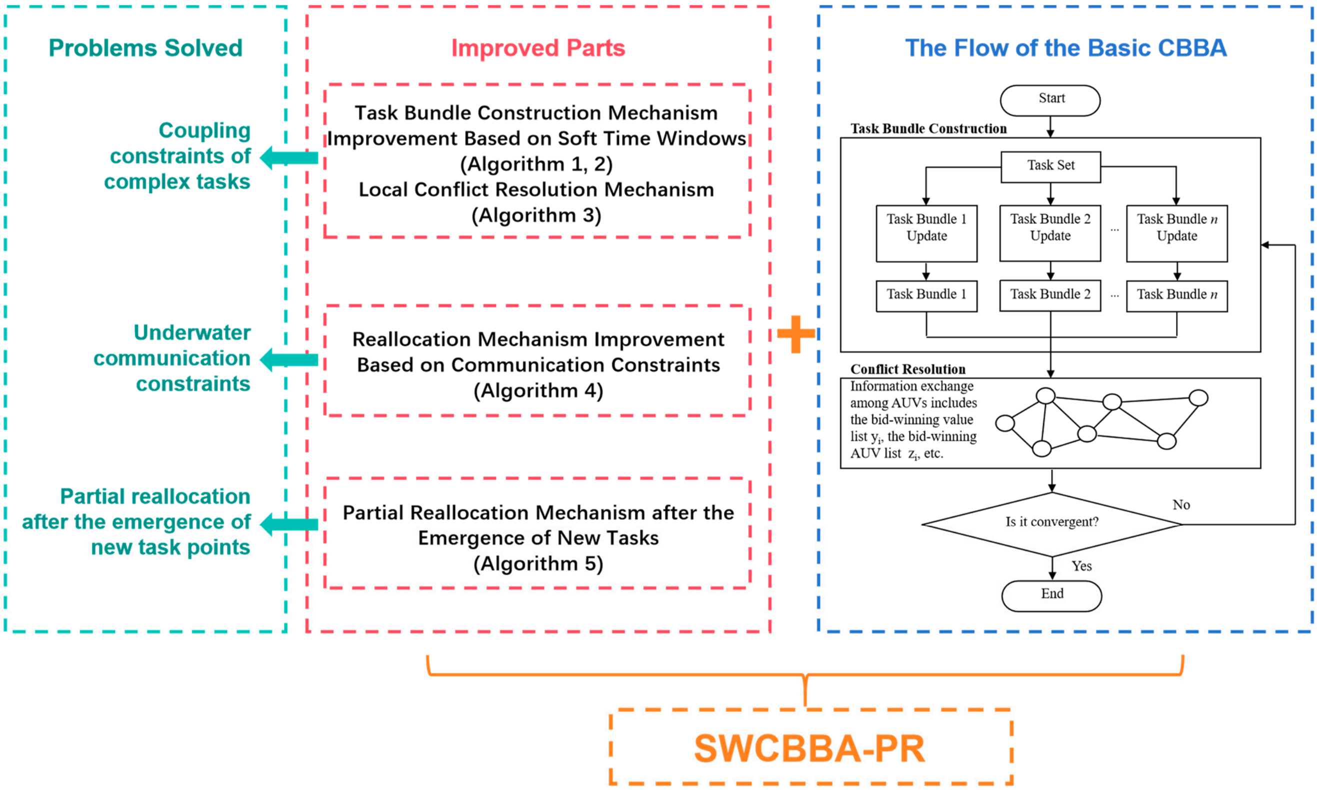

Figure 2. Explanatory diagram of the SWCBBA-PR algorithm architecture.

2. Problem Description and Modeling

2.1. Description of the Problem

When executing MCM tasks in practice, it is necessary to sequentially perform three subtasks: search, mine neutralization, and confirmation. In this paper, we mainly consider the task assignment scenario in which AUVs discover new suspicious task points within their detection range while performing the search subtasks of the MCM mission. The mission area is assumed to have N_A heterogeneous AUV, denoted as $A_i(i = 1, 2, \ldots, N_A)$, N_T known mission points and n^* unknown mission points. Multiple AUVs collaborate to perform the subtasks corresponding to each known task point, i.e., the search task T_j^S, the mine-neutralizing task T_j^E, and the confirmation task T_j^V have a total of N_t subtasks, and some AUVs will detect n^* unknown task points in the execution of the search subtasks, which is denoted as $T_j(j = 1, 2, \ldots, N_T + 3n^*)$, and each subtask can only be accomplished by one AUV with a matching type. Also, each AUV is capable of executing at most L_i tasks.

To ensure that $N_{\min}\underline{\underline{\Delta}}\min\{N_t + 3n^*, N_A L_i\}$ tasks are assigned at the same time, equalize the utilization efficiency of each AUV.

In order to more effectively solve the problem of task allocation for heterogeneous multiple AUVs, this paper will conduct task allocation for mission tasks in a two-dimensional marine environment. That is, all AUVs and task points are at the same depth and regarded as mass points. For the analysis in this paper, to enhance the adaptability of the task allocation model without losing generality, the following assumptions are proposed:

(1) The initial position information (x_i, y_i), speed information v_i, and power consumption per unit time e_i of all AUVs are known.
(2) The position information (x_j, y_j), fixed gain R_{j0}, initial gain R_j, time discount factor λ_j, and task execution duration of all task points are known.
(3) No account is taken of the collisions among AUVs.
(4) Every AUV has an equivalent probability of choosing any task.
(5) The resource-carrying capacity of each AUV is applicable to every task.
(6) The actual energy consumption during the navigation of an AUV is approximately linearly correlated with the distance it travels; thus, the concept of normalized energy consumption is employed.
(7) AUVs of the same type share identical basic conditions, including navigation speed and energy consumption.

In summary, the mission task allocation problem for heterogeneous multiple AUVs in the MCM scenario can be described as follows: In a two-dimensional plane, there are N_A available heterogeneous AUVs, N_T known task points to be allocated, and n^* unknown task points. Each task point consists of three subtasks: search, mine-neutralization, and confirmation, and each subtask needs to be completed by the corresponding type of AUV. By using the SWCBBA-PR algorithm proposed in this paper, the task execution sequence for each AUV is determined. This ensures that the task allocation scheme for heterogeneous multiple AUVs can satisfy the task timing coupling constraints while maximizing the total revenue and minimizing the total time cost.

2.2. Mathematical Modeling

2.2.1. Description of Heterogeneous Multi-AUV Systems and Mission-Coupling Constraints

The heterogeneity of multi-AUV systems is critically reflected in different functional characteristics and maneuvering performance:

(1) AUVs carry different resource payloads, such as sensors, cameras, anti-mine torpedoes, etc., to perform different types of subtasks. The matching matrix between AUVs and tasks is shown in Equation (1).

$$match_{ij} = \begin{cases} 1, & \mathrm{A_i \ can\ perform\ T_j} \\ 0, & \mathrm{otherwise} \end{cases} \tag{1}$$

(2) The differences in AUV maneuverability are reflected in different sailing speeds and standardized energy consumption. In addition, in the mission assignment results, the heterogeneous AUVs must not only satisfy the needs of the assigned mission tasks with their own mission execution capabilities but must also satisfy the relevant constraints that the mission tasks need to satisfy.

During an anti-mine mission, there are three subtasks that need to be performed at each mission point, i.e., the search subtask, the mine-neutralizing subtask, and the confirmation subtask. The task coupling constraints are reflected in three aspects:

(I) The anti-mine mission is considered accomplished only when all three subtasks are executed, so the total number of subtasks is $N_t = 3N_T$.

(II) The execution of subtasks should follow strict priority constraints, i.e., the mine-neutralizing subtask can only be executed after the search subtask has been completed, and the confirmation subtask can only be executed after the mine-neutralizing subtask has been completed.

(III) In practical applications, each subtask takes a certain amount of time to execute, and different subtasks have different execution times. Since the whole anti-mine task must be completed within a certain timeframe, a time window $\left[t_j^{start}, t_j^{last}, t_j^{end}\right]$ is introduced. t_j^{start} is the time when the task can start executing, t_j^{end} is the time when the task must finish executing. $t_j^{last} = t_j^{end} - t_j^{start}$ is the time window size for the task. $t_j^{duration}$ is the duration of executing the task. Assuming that the start time of the execution of the search subtask, the mine-neutralizing subtask, and the confirmation subtask are t_j^1, t_j^2, and t_j^3 respectively, and the durations are t_j^S, t_j^E, and t_j^V respectively, the conditions should be satisfied as follows:

$$t_j^{start} \le t_j^1 \le t_j^2 \le t_j^3 \le t_j^{end} \tag{2}$$

$$t_j^1 + t_j^S \le t_j^2 \tag{3}$$

$$t_j^2 + t_j^E \le t_j^3 \tag{4}$$

$$t_j^3 + t_j^V \le t_j^{end} \tag{5}$$

2.2.2. Objective Functions and Constraints

Considering the emergence of the new task point T^*, the partial task reassignment is modeled as follows:

(1) Global objective function

$$\max \sum_{i=1}^{N_A} \left(\sum_{j=1}^{N_t+3n^*} r_{ij}(x_i, p_i) x_{ij} \right) \tag{6}$$

$x_{ij}, x_{i(j+(N_t+3n^*)/3)}, x_{i(j+2(N_t+3n^*)/3)} \in \{0,1\}$ is the decision variable for task assignment, $x_{ij} = 1$ indicates that task j is performed by the i-th AUV, otherwise $x_{ij} = 0$. $p_i \in (\{1, \ldots, M\} \cup \{\varnothing\})^{L_i}$ is the sequence of paths for tasks performed by A_i. When the k-th element of p_i is $m \in \{1, \ldots, M\}$, it indicates that the k-th task point traveled to by the i-th AUV is the m-th task point, and when it is $\varnothing$, it indicates that the i-th AUV is assigned less than k tasks. $r_{ij}(x_i, p_i) \ge 0$ represents the gain that the i-th AUV gains from executing task T_j at the k-th position on its path, which is related to factors such as navigation distance cost and task completion time.

(2) Constraint conditions

Limit the maximum number of tasks that A_i can execute to L_i.

$$s.t. \sum_{j=1}^{N_t+3n^*} x_{ij} \le L_i, \quad \forall i = 1, \ldots, N_A \tag{7}$$

Limit the maximum total number of tasks that all AUVs can execute to $N_{\min}$.

$$\sum_{i=1}^{N_A} \sum_{j=1}^{N_t+3n^*} x_{ij} \le N_{\min} \underline{\underline{\Delta}} \min\{N_t + 3n^*, N_A L_i\} \tag{8}$$

Limit each task to be executed by a maximum of one AUV, and the task will only be considered completed after all subtasks at each task point have been executed.

$$\sum_{j=1}^{N_t+3n^*} x_{ij} \leq 1, \quad \forall i = 1, \ldots, N_A \tag{9}$$

$$\sum_{i=1}^{N_A} x_{ij} \leq 1, \quad \forall j = 1, \ldots, (N_t + 3n^*)/3 \tag{10}$$

$$\sum_{i=1}^{N_A} x_{i[j+(N_t+3n^*)/3]} \leq 1, \quad \forall j = 1, \ldots, (N_t + 3n^*)/3 \tag{11}$$

$$\sum_{i=1}^{N_A} x_{i[j+2(N_t+3n^*)/3]} \leq 1, \quad \forall j = 1, \ldots, (N_t + 3n^*)/3 \tag{12}$$

Task coupling constraint:

$$t_j^{start} \leq t_j \leq t_{j+(N_t+3n^*)/3} \leq t_{j+2(N_t+3n^*)/3} \leq t_j^{end} \quad \forall j = 1, \ldots, (N_t + 3n^*)/3 \tag{13}$$

$$t_j + t_j^S \leq t_{j+(N_t+3n^*)/3} \quad \forall j = 1, \ldots, (N_t + 3n^*)/3 \tag{14}$$

$$t_{j+(N_t+3n^*)/3} + t_j^E \leq t_{j+2(N_t+3n^*)/3} \quad \forall j = 1, \ldots, (N_t + 3n^*)/3 \tag{15}$$

$$t_{j+2(N_t+3n^*)/3} + t_j^V \leq t_j^{end} \quad \forall j = 1, \ldots, (N_t + 3n^*)/3 \tag{16}$$

Power limit:

$$\frac{L(p_i)}{v_i} e_i \leq E_i \quad \forall i = 1, \ldots, N_A \tag{17}$$

The initial power of the multi-AUV system is assumed to be $E = \{E_1, E_2, \ldots, E_{N_A}\}$, and $L(p_i)$ denotes the sailing distance for A_i to perform the task along the path p_i. Thus, the energy consumption of the task allocation scheme for A_i to execute the corresponding task sequence voyage must not exceed its initial power.

Under multiple constraints, it is necessary to dynamically adjust the task bundles of multiple AUV systems based on the emergence of new tasks to achieve an optimal task allocation scheme with maximum comprehensive gains. The algorithm enhances the flexibility and efficiency of the system, ensuring rational task assignment and the best execution results.

3. SWCBBA-PR Algorithm

Currently, the commonly used improved CBBA algorithms for the task assignment problem arising from new tasks are the no-reset consensus-based bundle algorithm (CBBA-NR), the single-task reset consensus-based bundle algorithm (CBBA-SR), and the full-reset consensus-based bundle algorithm (CBBA-FR). To ensure the speed of the CBBA-NR algorithm, the previously assigned task plan is not reset. Although the convergence is almost unaffected by new tasks, the flexibility of the algorithm is limited, especially in complex, constrained scenarios. If AUVs have payload resource constraints or only a few AUVs can perform specific tasks, the AUVs that can perform the new task T^* may not have sufficient resources to perform T^*; thus, they are unable to guarantee the optimal task allocation plan. In order to solve the problem of new tasks not being assigned due to insufficient resources in CBBA-NR, CBBA-SR will reset the last task added to the task bundle, which is also the one with the lowest gain value, and reassign the task. However, it does not consider the relationship between the new task and the AUV type and the original task allocation scheme. In dynamic environments, when the situational awareness changes significantly, CBBA-FR re-solves the new task allocation problem by re-running CBBA.

However, the disadvantage of this algorithm is that in a task assignment scenario with n_t tasks and a communication topology network of diameter D, the new task response time for a single task is $O(n_t D)$. Moreover, CBBA-FR ignores the already obtained conflict-free solutions, wastes the computation and communication used to allocate the original tasks, and does not guarantee the convergence of the original task allocation problem. In order to better balance the quality of task allocation and convergence speed, this paper designs SWCBBA-PR, which allows each AUV to reset a portion of its existing allocation scheme after a new task point is discovered and then reallocates it.

3.1. Algorithm Key Elements

In the SWCBBA-PR algorithm, the first step is to explicitly define the crucial elements of the task assignment information for the i-th AUV:

(1) Task bundle list b_i

$$b_i \underline{\underline{\Delta}} \left\{ b_{i1}, \ldots, b_{i|b_i|} \right\} \tag{18}$$

The task bundle list b_i is the task bundle assigned to the i-th AUV. The tasks in the list are assigned in order of the tasks added. $|b_i|$ is the length of the task bundle list, i.e., the maximum number of tasks assigned to each AUV, and $b_i = \varnothing$ means that the task bundle is empty.

(2) Path list p_i

$$p_i \underline{\underline{\Delta}} \left\{ p_{i1}, \ldots, p_{i|p_i|} \right\} \tag{19}$$

The path list p_i is the bundle of path sequences for the i-th AUV pending task, and the task sequences are arranged based on the execution order during the task assignment process. $|p_i|$ is the length of the path list, $p_i = \varnothing$ means the path list is empty.

(3) Winning bid value list y_i

$$y_{ij} \in y_i (j = 1, 2, \ldots, N_T) \tag{20}$$

It indicates the highest bid for the task T_j from each AUV, derived from the information exchanges of A_i with its fellow AUVs. However, $y_{ij} = 0$ when A_i believes that T_j does not have a winning bidder.

(4) Winning AUV list z_i

$$z_{ij} \in z_i (j = 1, 2, \ldots, N_T) \tag{21}$$

$z_{ij} = 1$ denotes that the corresponding AUV that the i-th AUV considers to have the highest bid for the task T_j is the i-th AUV, otherwise $z_{ij} = 0$.

(5) Timestamp list s_i

$$s_i \underline{\underline{\Delta}} \{ s_{i1}, \ldots, s_{iN} \} \tag{22}$$

The timestamp list s_i records the moment at which A_i gets updated information from the rest of the AUVs in the trusted communication range, where s_{ik} indicates the moment when A_i gets the latest information from A_k, as specified in the update rule in Equation (23). This list is a key element of communication in the conflict resolution phase.

$$s_{ik} = \begin{cases} \tau_r & g_{ik} = 1 \\ \max\limits_{l:g_{il}=1} s_{lk} & \text{otherwise} \end{cases} \tag{23}$$

Here, $g_{ik} = 1$ indicates that A_i lies within the reliable communication range of A_k, while $g_{ik} = 0$ in other cases. τ_r is the time at which A_i gets the message.

3.2. Improved Task Bundle Construction Phase

Given the energy consumption and limited maximum operating range of AUVs in a practical environment, a refined marginal function $S_i^{p_i}$ is developed.

$$S_i^{p_i} = \sum_{j \in p_i} \left(e^{-\lambda_j (t_{ij} - t_{start})} R_j u(t_{ij}) - e_i \frac{\Delta D_{ij}}{v_i} \right) \tag{24}$$

$$u(t_{ij}) = \begin{cases} 1 & t_j^{start} \le t_{ij} \le t_j^{end} \\ 0 & \text{otherwise} \end{cases} \tag{25}$$

$\lambda_j < 1$ represents the time discount factor. t_{ij} is the execution time of the task T_j in the A_i path bundle list p_i. R_j is the initial gain of being assigned to complete the task T_j at the start time, with the first term decreasing as the actual start time of the task increases from the initial start time. The exponential function is chosen here because it has a smooth variation characteristic, which can reflect the impact of task time changes on gains more delicately. Compared to some simple linear functions, it is closer to the complexity of time value changes in tasks in reality. $u(t_{ij})$ is the binary variable that checks whether t_{ij} meets the time window condition as depicted in Equation (25). e_i is the normalized power consumption per unit time, and ΔD_{ij} is the distance from A_i to task T_j.

In the multi-AUV cooperative mission tasking problem, the marginal function in Equation (24) is composed of the time discount gain minus the power cost. This makes the marginal function a DMG function. The introduction of the marginal function achieves the convergence of the conflict-free allocation.

Nevertheless, this refined specification of the marginal function harbors a potential drawback. In certain situations, due to the slow movement of AUVs in underwater environments, the time discount gain may be less than the electricity cost, resulting in a negative marginal function result. Consequently, task T_j will not be selected during the task package construction phase, thus failing to achieve the goal of improving the task allocation rate. Therefore, Equation (26) is modified.

$$S_i^{p_i} = \sum_{j \in p_i} \left(R_{j0} + e^{-\lambda_j (t_{ij} - t_{start})} R_j u(t_{ij}) - e_i \frac{\Delta D_{ij}}{v_i} \cdot 0.1 \right) \tag{26}$$

R_{j0} is the fixed gain of the task T_j. To balance the fixed gain with the initial gain, the voyage cost term is multiplied by 0.1. Also, in order to maximize the participation of AUVs in the task, it should be ensured that $S_i^{p_i} > 0$. Thus, R_{j0} should satisfy the following:

$$R_{j0} > e_i \Delta D_{ij} - e^{-\lambda_j (t_{ij} - t_{start})} (R_j - R_{j0}) u(t_{ij}) \ge e_i \frac{\Delta D_{ij}}{v_i} \tag{27}$$

The refined marginal function takes into account the heterogeneity of AUVs. Firstly, AUVs of various types have distinct navigation velocities, which leads to varying arrival times at the target. Secondly, AUVs of different types feature different levels of standardized power consumption.

Since the task coupling constraint also involves the temporal coupling relationship between tasks, a soft time window is employed to update the task start time dynamically to address this issue. The mechanism of task-specific soft time window updating is presented in Algorithm 1.

Algorithm 1. SWCBBA-PR: task soft time window update mechanism in the *t*-th iteration

Inputs: list of winning AUVs at the *t*-th iteration $z_i(t)$, task start time t_j^{start}, execution time $t_j^{duration}$.
Output: updated task start time t_j^{start}.
for $j = 1$ to N_t do
  if $i \leq N_A$ makes $z_{i(j-N_t/3)}(t) = 1$ do
    $t_j^{start} = t_{j-N_t/3}^{start} + t_{j-N_t/3}^{duration}$
  end
end for

To meet the complex task coupling constraints, each AUV needs to update $match_{ij}$ before constructing a task bundle to ensure that the resulting task allocation scheme satisfies the resource constraints of a heterogeneous multi-AUV system. During initialization, the start time of the lower-level task is the specified end time of the upper-level task. After the algorithm starts running, it determines whether the upper-level task has been assigned. This determination is based on the AUV list $z_i(t)$ obtained at the *t*-th iteration. If it has been assigned, the end time of the upper-level task is used as the start time of the lower-level task, and the task timing constraint is transformed into a task soft time window constraint.

Consequently, Algorithm 2 describes the enhanced phase of task bundle construction.

Algorithm 2. SWCBBA-PR: task bundle construction phase for the *i*-th AUV in the *t*-th iteration

Input: the result at the (t−1)-th iteration $b_i(t-1), p_i(t-1), y_i(t-1), z_i(t-1), s_i(t-1), t_j^{start}, t_j^{duration}$.
Output: the result at the *t*-th iteration $b_i(t), p_i(t), y_i(t), z_i(t), s_i(t), t_j^{start}$.
1: $b_i(t) = b_i(t-1), p_i(t) = p_i(t-1), y_i(t) = y_i(t-1), z_i(t) = z_i(t-1), s_i(t) = s_i(t-1)$
2: while $|b_i(t)| \leq L_i$ do
3: $c_{ij}(b_i) = \max\limits_{n \leq |p_i|} S_i^{p_i \oplus_n \{j\}} - S_i^{p_i}, \quad \forall T_j \in T \backslash b_i$
4: $h_{ij} = II(c_{ij} > y_{ij}) \quad \forall j \in N_T$
5: $J_i = \mathrm{argmax}_j (c_{ij}(b_i) \times h_{ij})$
6: $n_{i,J_i} = \mathrm{argmax}_j S_i^{p_i \oplus_n \{J_i\}}$
7: $b_i = b_i \oplus_{end} \{J_i\}, p_i = p_i \oplus_{n_{i,J_i}} \{J_i\}$
8: $y_{i,J_i}(t) = c_{i,J_i}, z_{i,J_i}(t) = i$
9: Update the task time window in accordance with Algorithm 1
10: end while

Line 9 has been added to the base CBBA algorithm in order to satisfy the task coupling constraints while $u(t_{ij})$ of Equation (25) has been added to the marginal function in line 3. This is done so that only task solutions satisfying the timing constraints can be added to the task bundles. Added in an optimal position, they should have non-negative marginal gains.

In summary, the improved mission bundle construction phase with a soft time window update mechanism can select mission scenarios. These scenarios are for heterogeneous multi-AUV systems and satisfy the AUV characteristics and mission coupling constraints in the MCM mission scenario.

3.3. Improved Conflict Resolution Stage

To address the complex task coupling constraints, the conflict resolution phase is divided into local conflict resolution and global conflict resolution. The global conflict resolution stage is the conflict resolution stage in the CBBA algorithm. The specific process of resolving local conflicts is presented in Algorithm 3.

Algorithm 3. SWCBBA-PR: local conflict resolution phase for the *i*-th AUV in the *t*-th iteration

Input: result to be updated in the *t*-th iteration $y_i(t), z_i(t), s_i(t)$ and sender's message $y_k(t), z_k(t), s_k(t)$
Output: Update results for the *t*-th iteration $y_i(t), z_i(t), s_i(t)$
1: for $T_j \in b_i$ do
2: if $j \leq N_t/3$ do %Update assignment information for search subtasks
3: Updated in accordance with CBBA conflict resolution rules $y_i(t), z_i(t), s_i(t)$
4: else if $j \leq 2N_t/3$ and $s_{i(j-N_t/3)}(t) = s_{k(j-N_t/3)}(t)$ do %Update the assignment of the mine-neutralizing subtasks
5: Updated in accordance with CBBA conflict resolution rules $y_i(t), z_i(t)$
6: else if $s_{i(j-2N_t/3)}(t) = s_{k(j-2N_t/3)}(t)$ do %Update the assignment information of the confirming subtasks
7: Updated in accordance with CBBA conflict resolution rules $y_i(t), z_i(t)$
8: else
9: $y_{ij}(t) = 0, z_{ij}(t) = \varnothing, s_{ij}(t) = 0$
10: $y_{i(j-N_t/3)}(t) = 0, z_{i(j-N_t/3)}(t) = \varnothing, s_{i(j-N_t/3)}(t) = 0$
11: $y_{i(j-2N_t/3)}(t) = 0, z_{i(j-2N_t/3)}(t) = \varnothing, s_{i(j-2N_t/3)}(t) = 0$
12: end
13: end
14: end
15: end for

From Algorithm 3, it can be seen that in order to satisfy the task coupling constraints of the MCM mission scenario, the assignment of the mine-neutralizing subtask is constrained by the assignment of the search subtask, while the assignment of the confirmation subtask is constrained by the assignment of the mine-neutralizing subtask. Lines 2–3 indicate that the search subtask is a first-level subtask and is not constrained by any other subtasks. Thus, the local conflict resolution phase of the search subtask is only influenced by the communication message update. Lines 4–7 indicate that when the allocation information for the upper-level subtasks is consistent, the allocation information for the lower-level tasks will be updated according to the CBBA conflict resolution rules. Otherwise, all subtasks related to this upper-level task in the task bundle will be released. Therefore, the local conflict resolution phase can ensure that the task allocation scheme satisfies the coupling constraints of task timing.

3.4. Improved Task Reassignment Program

Due to the limited trusted communication range, SWCBBA-PR's core concept is to convert the overall allocation process into multiple static task allocations at discrete time steps; that is, the motion process of a multi-AUV system is discretized and processed by the time step T. When $T = 0$, the AUV converges to a task allocation scheme with partial conflicts based on its own and the initial position information of the task, constrained by the trusted communication range D_{cd}, by iterating between the task packet construction stage and the conflict resolution stage. As the discrete time step increases towards the current mission-goal location, all individual AUVs follow the planned mission sequence and path. The topological state of the communication network of the AUV cluster changes when different AUVs enter the communication range, or the task state changes when the task is completed. Based on its own and the current status of the task, the AUV exchanges intermediate and winning AUV information with fellow AUVs present in its communication coverage area, resolves task conflicts in previous allocation schemes, then reassigns tasks and updates the discrete time step $T \rightarrow T+1$. It iterates until all AUVs complete all tasks in their task bundle or exceed the maximum task completion time $T_{\max}$. The detailed procedure is described in Algorithm 4.

Algorithm 4. SWCBBA-PR: trusted communication throughput map altered task reassignment scheme

Input: $T=0, G(0)=O, POS_i(0), POS_j, p_i(0)=\varnothing, T_{\max}$.
Output: the result of the task assignment b_i, p_i, y_i, z_i, s_i.
1: while $T < T_{\max}$ and $T=0$ or $p_i(T) \neq \varnothing$ do
2: for $i=1$ to N_A do
3: for $k=1$ to N_A do
4: if $i \neq k$ and $D(A_i, A_k) \leq (D_{cd}/2)$ do
5: $g_{ik}(T)=1$
6: $g_{ki}(T)=1$
7: else
8: $g_{ik}(T)=0$
9: $g_{ki}(T)=0$
10: end
11: end for
12: end for
13: if $G(T) \neq G(T-1)$ do
14: for $i=1$ to N_A do
15: Using CBBA to reallocate unallocated tasks in the new trusted communication graph
16: end for
17: end
18: for $i=1$ to N_A do
19: $T_j = p_i^i(T)$
20: if $D(A_i, T_j) \leq |v_i(T)| \cdot \Delta T$ do
21: $p_i(T+1) = p_i^{2:|p_i|}(T)$
22: $POS_i(T+1) = POS_j$
23: else
24: $POS_i(T+1) = POS_i(T) + v_i(T)\Delta T$
25: end
26: end for
27: $T=T+1$
28: end while

In Algorithm 4, T is the discrete time step, G is the trusted communication topology map of the AUV cluster, $POS_i(T)$ denotes the real-time location of A_i, POS_j denotes the location of the task T_j, and p_i denotes the real-time path sequence of A_i. Lines 2–12 demonstrate that at every discrete step, the AUV cluster needs to update its trust-based communication topology map determined by distance. Lines 13–17 indicate that when the communication topology map changes, the AUV cluster will perform partial task reassignment. Tasks completed or in progress before the discrete step T must be the optimal plans. This is because they result from communication and conflict resolution with other AUVs. Therefore, each reallocation only involves tasks that were unassigned before the discrete step T. AUVs engaged in task execution do not participate in the reallocation phase, preventing duplicate allocation. Lines 18–26 show that during every discrete time step, every AUV will follow its pre-planned route to update its location.

3.5. Partial Reset Mechanism Design

For the above task scenarios, a partial reset mechanism is introduced. First, a reset task candidate set J_i^{reset} is established. This is based on the relationship between the time and location of the discovery of the new task point and the time series and distance of the original task allocation result. Second, n_i^{reset} tasks with the lowest return value are selected for reset and denoted as T_i^{reset}. Also, the lower-level tasks related to T_i^{reset} are reset. Then, constraint-violation tasks and task conflicts are resolved through local and global conflict resolution stages. Meanwhile, the size of n_i^{reset} can be adjusted by integrating the number of new tasks and the response speed requirement.

The specific algorithm for the partial reset mechanism is presented in Algorithm 5.

Algorithm 5. SWCBBA-PR: partial reset mechanism for the *i*-th AUV in the *t*-th iteration

Input: the result in the $(t-1)$-th iteration $b_i(t-1), p_i(t-1), y_i(t-1), z_i(t-1), s_i(t-1)$.
Output: the input $b_i(t), p_i(t), y_i(t), z_i(t), s_i(t)$ in the *t*-th iteration.
1: $b_i(t) = b_i(t-1), p_i(t) = p_i(t-1), y_i(t) = y_i(t-1), z_i(t) = z_i(t-1), s_i(t) = s_i(t-1)$
2: $n_i^{reset} = \frac{t_{res}}{2 \cdot t_{com}} + \frac{n_i^*}{2}$
3: if $match_{i*} = 1$ do
4: $\quad J_i^{reset} = \varnothing$
5: $\quad$ for $T_j \in b_i(t)$ do
6: $\quad\quad$ if $\left(t_*^{start} > t_{ij} + \frac{\Delta D_{j*}}{v_i}\right)$ or $\left(t_*^{end} + \frac{\Delta D_{j*}}{v_i} < t_{ij}\right)$ do
7: $\quad\quad\quad$ if $\Delta D_{j*} < D_{reset}$ do
8: $\quad\quad\quad\quad J_i^{reset} = J_i^{reset} \cup \{j\}$
9: $\quad\quad\quad$ end if
10: $\quad\quad$ end if
11: $\quad$ end for
12: $\quad y_i^{sort}(t) = Sort\left(y_i^{reset}(t)\right)$
13: $\quad T_i^{reset} = \left\{ j \in J_i^{reset} \middle| y_{ij}^i \in y_i^{sort}(t)\left[1 : n_i^{reset}\right] \right\}$
14: $\quad$ for $j \in T_i^{reset}$ do
15: $\quad\quad b_i(t) = b_i(t)/j, p_i(t) = p_i(t)/j$
16: $\quad\quad y_{ij}(t) = 0, z_{ij}(t) = \varnothing, s_{ij}(t) = 0$
17: $\quad\quad y_{i(j-N_t/3)}(t) = 0, z_{i(j-N_t/3)}(t) = \varnothing, s_{i(j-N_t/3)}(t) = 0$
18: $\quad\quad y_{i(j-2N_t/3)}(t) = 0, z_{i(j-2N_t/3)}(t) = \varnothing, s_{i(j-2N_t/3)}(t) = 0$
19: $\quad$ end for
20: end if

The t_{res} in line 2 is the response speed required by the new task point. It can be seen that the size of n_i^{reset} combines the number of new tasks and the response speed requirement. In line 3, A_i determines whether to participate in the partial reset mechanism based on the matching matrix $match_{i*}$ between AUVs and tasks. Only AUVs capable of performing the new task T^* undergo partial reset. Lines 4–11 aim to avoid unnecessary computational complexity by establishing a reset task candidate set J_i^{reset}, which includes tasks with execution time coinciding with the time when the new task T^* was discovered, and the end time $[t_*^{start}, t_*^{end}]$, as well as tasks that are less than D_{reset} away from the new task point. Line 12 ranks the tasks in the task alternative set J_i^{reset} according to their gain value in the list of winning values $y_i(t)$, and in line 13, the n_i^{reset} task with the smallest gain value, i.e., T_i^{reset}, is selected as the reset task since the optimal insertion location of the new task has a high probability of being either before or after the distance from the execution of the nearest task. Lines 14–19 reset T_i^{reset}, and also reset the lower-level tasks coupled to this upper-level task to ensure compliance with MCM task coupling constraints.

As can be seen in Algorithm 5, after the discovery of the new task point T^*, a reset task alternative set J_i^{reset} is created. This set is formed from the tasks in the original assignment scheme task bundle. The creation is based on the relationship between the time and place where the new task point was discovered and the time series and distance from the original task assignment result. The task is reset by deleting tasks from $b_i(t)$ and $p_i(t)$ and resetting the values in $y_{ij}(t)$ and $z_{ij}(t)$. The aim is to achieve better resource allocation by reallocating existing tasks while still ensuring the convergence of the algorithm. n_i^{reset} can be adjusted to adapt to the response time required for the new task. In addition, SWCBBA-PR only selects AUVs that are compatible with the new task type to participate in reassignment. This can reuse the original allocation in $z_i(t)$ and ensure that no reset tasks are "wasted" on AUVs that did not participate in reassignment. Meanwhile, the algorithm can choose to reset only some tasks based on the time series and distances between new task points and original task assignments. It continues to utilize $y_i(t)$ and $z_i(t)$ to achieve replanning within the desired convergence range.

The flowchart of the SWCBBA-PR algorithm is depicted in Figure 3, and the step-by-step instructions are as follows:

Step 1: Initialize the task allocation system, which includes:

(1) Initialize the clock so that all AUVs share a common zero-time instant.
(2) Initialize AUV parameters, such as initial coordinates, speed, and equipment information.
(3) Initialize task information, mainly task coordinates, time windows, and type information. Multiple AUVs wait at their initial coordinate positions before receiving commands.

Step 2: Establish a communication topology among all AUVs to ensure the accurate sending and receiving of task bundles and execution status.

Step 3: Each AUV conducts task allocation according to the communication reallocation consensus-based bundle algorithm with a soft time window. Consider the task coupling constraints of MCM mission. Introduce the parameter of timestamp. Design local and global conflict resolution stages to resolve conflicts in the task allocation results. Send the time information and the optimized task bundles of each AUV to the AUVs within the trusted communication range.

Step 4: Each AUV follows the allocated task bundle and goes to each suspicious point in sequence to execute tasks. The AUV updates its position according to the set discrete time. When the communication topology among AUVs changes, re-allocate the tasks that have not been allocated before time T according to the actual situation, and then execute the tasks.

Step 5: If new task points emerge, establish a reset task alternative set based on their temporal and distance relationships with the original task allocation plan. Select the n_i^{reset} tasks with the lowest gain value from the set for reallocation to obtain a new task allocation plan and then continue to execute tasks.

Step 6: After exceeding the maximum task completion time $T_{\max}$ or all tasks in the task package have been completed, the entire task execution process ends.

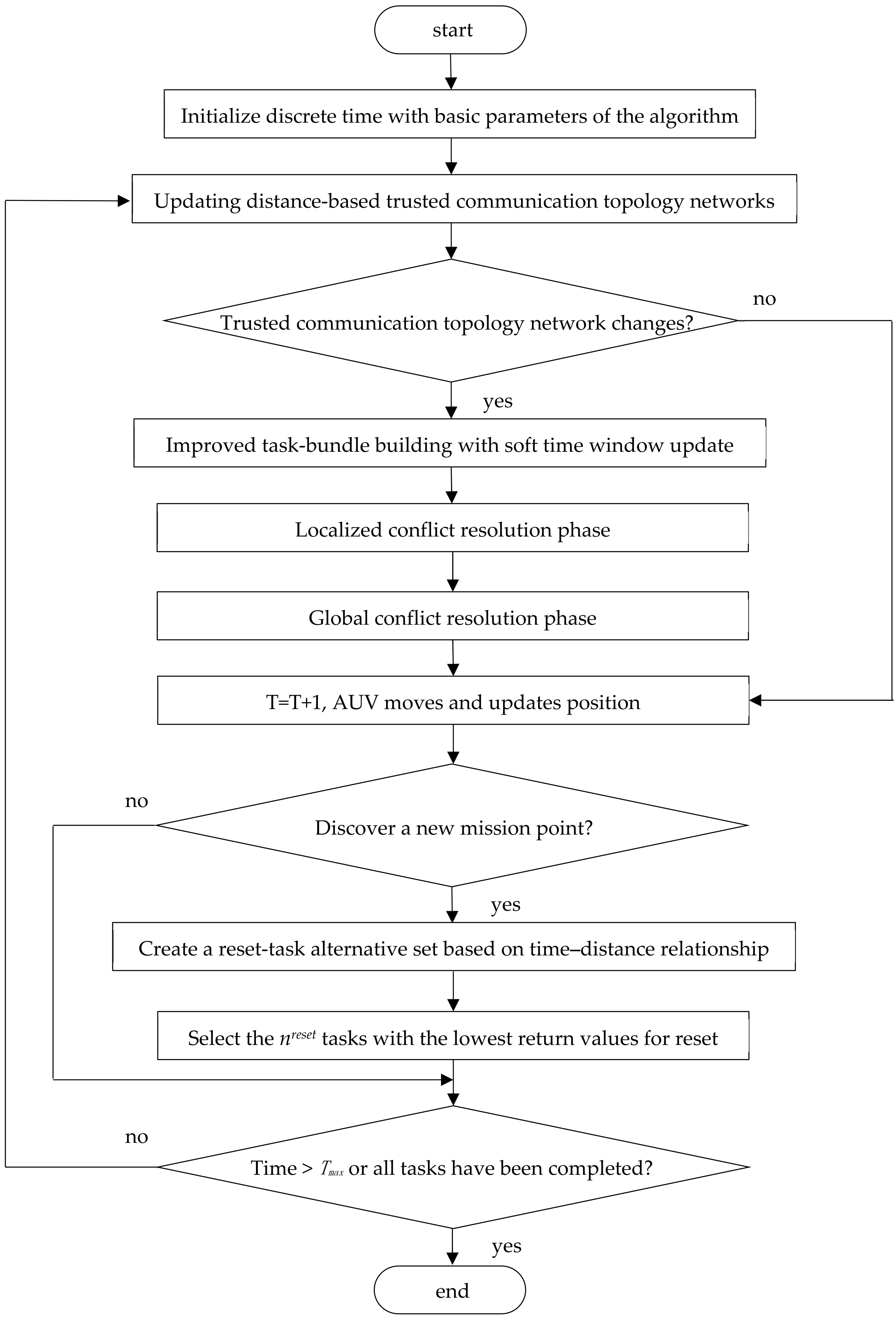

Figure 3. Flowchart of the SWCBBA-PR algorithm.

3.6. Convergence Analysis of the SWCBBA-PR Algorithm

The premise for SWCBBA-PR to generate feasible and conflict-free task allocation schemes that satisfy complex constraints is that the marginal function in the task package construction phase should satisfy the DMG condition. Resetting n_i^{reset} tasks without selection or using CBBA-NR or CBBA-FR algorithms may result in reassigned tasks not meeting the DMG conditions. This may lead to the inability to ensure convergence or obtain conflict-free task allocation schemes.

Therefore, a key requirement for SWCBBA-PR to select the tasks to be used for reset is that T_i^{reset} must be the task with the lowest gain value in each AUV task bundle. This ensures that the marginal function satisfies the DMG condition, guaranteeing the convergence of the SWCBBA-PR algorithm. If task resets are performed in other orders (such as random selection or highest bid), the algorithm cannot achieve decreasing bids and converge to a conflict-free solution.

As a result, each AUV in SWCBBA-PR resets only the n_i^{reset} tasks in the task bundle with the lowest gain value, and the algorithm can converge to a conflict-free task assignment solution in finite time. While SWCBBA-PR is more stable compared with CBBA-FR in terms of convergence, there is no guarantee that performance will improve in the worst case. Suppose there is only one task that needs to be reset for an AUV, and that task happens to be the first one in the task bundle of the original allocation scheme, it may lead to complete replanning.

However, if the algorithm converges on the first N_t tasks before the new task T^* is discovered, then it can ensure a worst-case performance of $O(n^{reset} D_{cd})$, where $n^{reset} = N_A n_i^{reset}$ denotes the total number of tasks that need to be reset for a multi-AUV system. In this case, the algorithm can then select the lowest bid task from the entire multi-AUV system. Since the algorithm has reached a consensus on the initial task allocation scheme, these n^{reset} lowest-bid-value tasks are actually the last n^{reset} tasks allocated during the task bundle construction phase. As higher-value tasks continue to be assigned, the algorithm is able to converge within $O(n^{reset} D_{cd})$ communication rounds after the partial reset.

4. Simulation Results and Analysis

Simulate and validate the designed SWCBBA-PR algorithm in the process of discovering new suspicious task points during the search, mine neutralization, and confirmation tasks of light and heavy AUVs to complete anti-mine missions. Section 4.1 validates the feasibility of SWCBBA-PR and Section 4.2 validates the algorithm performance under different discovery conditions during the execution of search subtasks and compares it with the introduction of SWCBBA-NR and SWCBBA-FR.

Within a two-dimensional area of 1 km $\times$ 1 km, heterogeneous AUV clusters need to perform search, mine neutralization, and confirmation subtasks on multiple suspicious task points within [0, 3000] seconds, i.e., the maximum discrete time step is $T_{\max}$ = 3000 s. The maximum number of tasks that an AUV can execute is $L_i = 8$, and the fixed gain $R_{j0} = 150$. For the sake of demonstration, the T_{10} task point is taken as a newly discovered task point randomly found when the AUV performs the search subtasks of other task points. The parameter settings for heterogeneous AUVs and various types of subtasks are shown in Tables 1 and 2, respectively. The matching table of heterogeneous AUVs and various types of subtasks is presented in Table 3.

Table 1. Heterogeneous AUV parameters.

AUV Type	Speed v_i (m/s)	Range C_i (m)	Standardized Power Consumption e_i
Light AUV A_1–A_3	2	5000	1
Heavy AUV A_4–A_6	2	10,000	2

Table 2. Subtask parameters.

Subtask Type	Execution Time $t_j^{duration}$ (s)	Initial Gain R_j	Time Discount Factor λ_j
Search subtasks T_1–T_{10}	120	200	0.1
Mine-neutralizing subtasks T_{11}–T_{20}	180	300	0.1
Confirmation subtasks T_{21}–T_{30}	120	200	0.1

Table 3. AUV and subtask matching table.

Whether the AUV Can Perform Subtasks		Subtask Type		
		Search Subtasks	Mine-Neutralizing Subtasks	Confirmation Subtasks
AUV type	Light AUV	yes	no	yes
	Heavy AUV	no	yes	no

Based on the above parameters, the performance of SWCBBA-PR is verified from several aspects.

4.1. Feasibility Verification of the SWCBBA-PR Algorithm

For the convenience of simulation effect display, six heterogeneous AUVs are set to perform anti-mine tasks on nine known suspicious task points, i.e., searching, mine neutralization, and confirming a total of $N_t = 27$ subtasks. When executing a random search subtask, a new suspicious task point, T_{10}, is discovered. The starting positions of AUVs and the locations of known tasks are randomly dispersed across the task zone, and the positions of new suspicious task points are randomly distributed within the detection range of 45.72 m of the detection sonar carried by the lightweight AUV. The start time of the known task is randomly allocated by the system, and the start time of the new task is the end time of the search subtask that discovered it. AUVs have a trusted communication distance of 400 m, which means D_{cd} = 400 m. In Figures 4–7 blue, green, and red represent the search subtask, mine neutralization subtask, and confirmation subtask, respectively. In the left subfigure, blue represents the light AUV and green represents the heavy AUV.

When the discrete time step T = 0, the task paths and task timing assigned to each AUV are presented in Figure 4. In the initial allocation result, some AUVs are not within the trusted communication range, leading to the redundant assignment of tasks T_{13}, T_{14}, T_{15}, T_{18}, T_{19}, T_{26}, and T_{27}. Due to the repeated allocation occupying the AUV task package, one search subtask was not assigned, resulting in subsequent mine neutralization and confirmation subtasks being unassignable. From the graph, it can be seen that although the task allocation scheme satisfies the task coupling constraints of MCM mission task allocation, the collaborative effect of multiple AUVs is poor, with a task allocation rate of only 85.19%, a suspicious task point resolution rate of only 77.78%, and a global total gain of only 5571.40.

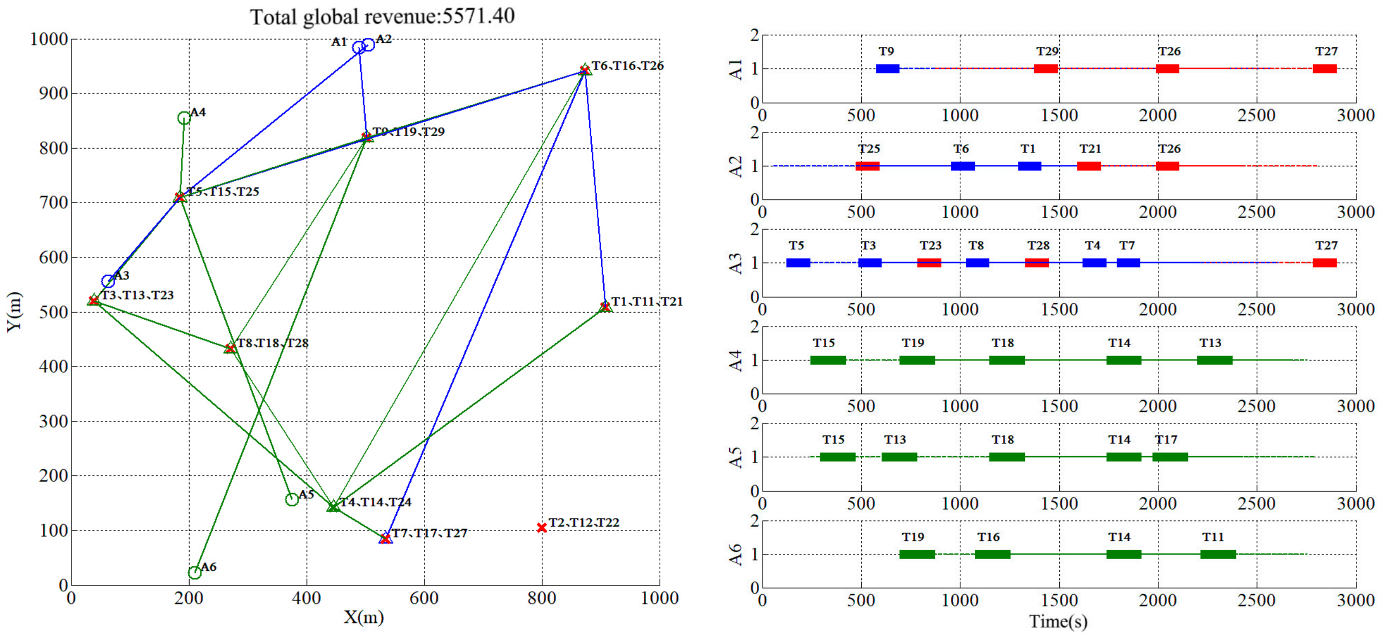

Figure 4. Schematic of the task allocation result plane with task timing diagram at T = 0.

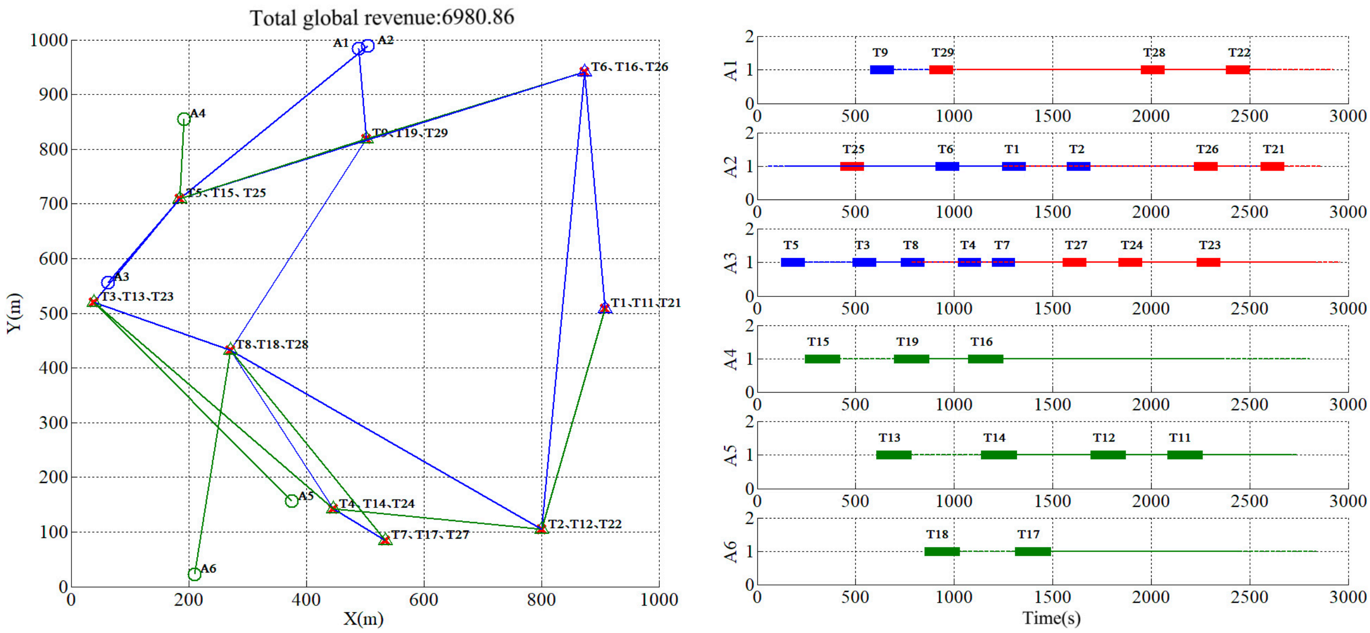

Figure 5. Schematic plan of tasking results before discovery of new tasking points with task timing diagrams.

Before and after the new task discovery, i.e., before and after the execution of the partial task reset mechanism, the task paths assigned by each AUV and the timing of the specific executed tasks are shown in Figures 5 and 6, respectively. From Figure 5, it can be seen that as the discrete time T increases, through the SWCBBA-CR algorithm for reallocation, there is no task reallocation in the task allocation results, and the global total gain is also higher than the initial allocation, which is 6980.86. From Figure 6, after the execution of the T_3 searching subtask, a new suspicious task point T_{10} is found within the detection range, with its start time being the end time of T_3 execution. As the new task point is discovered, A_1, A_2, and A_3 with corresponding task execution capability will participate in the execution of the partial task reset mechanism. Firstly, based on whether the task start time overlaps with the task time sequence before the discovery of the new task point and the relationship between the distance of the new task point and the other task points, the reset task alternative set $J_1^{reset} = \{T_9\}$, $J_3^{reset} = \{T_8, T_4, T_7\}$ is established. Among them, A_2 has no alternative reset task because the task execution time of T_6 and T_1, although coinciding with the new task time window, is too far away from the new task point and, therefore, not included in the reset task candidate set. Secondly, the number of new tasks $n^* = 1$ and the response speed requirement t_{res} = 150, t_{com} = 50 are combined to determine n_i^{reset} = 2, and then the n_i^{reset} task with the lowest gain value,$T_1^{reset} = \{T_9\}$, $T_3^{reset} = \{T_8, T_4\}$, is selected from J_1^{reset} and J_3^{reset} for reset. In addition, in order to ensure that the MCM task coupling constraints are satisfied, the lower-level tasks that are coupled to this upper-level task, i.e., T_{14}, T_{18}, T_{19}, T_{24}, T_{28}, T_{29}, are also reset.

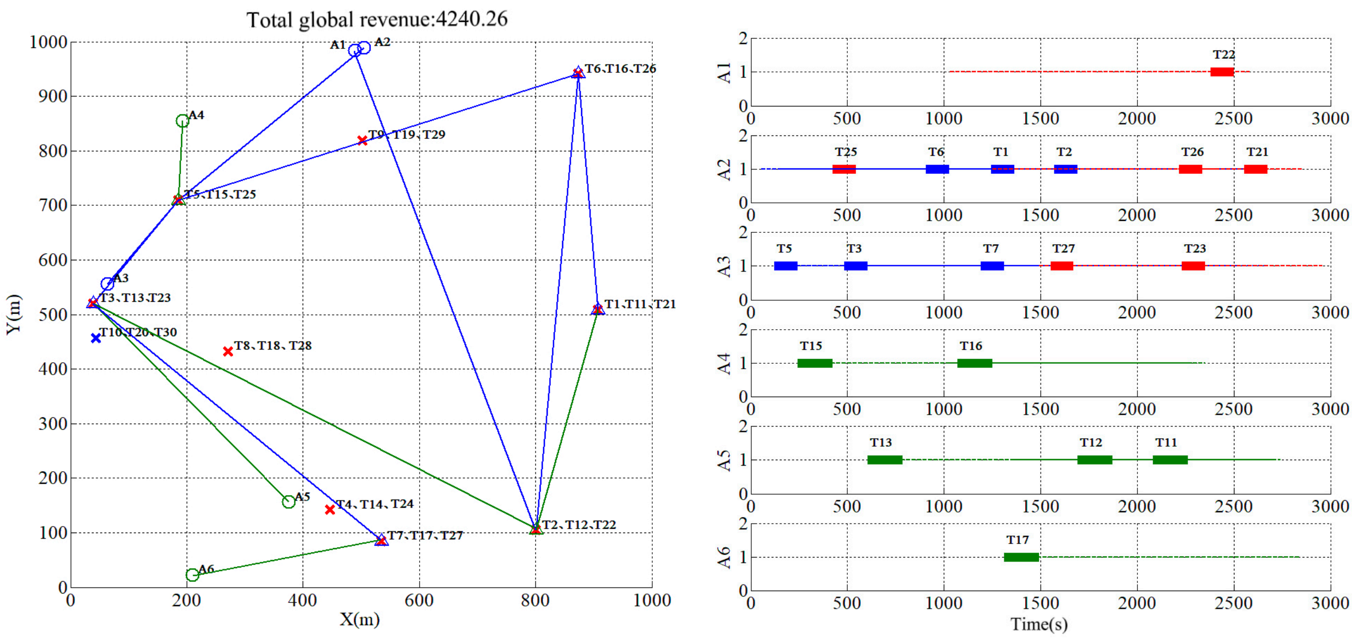

Figure 6. Schematic diagram of the plane with task timings after task reset after new task point discovery.

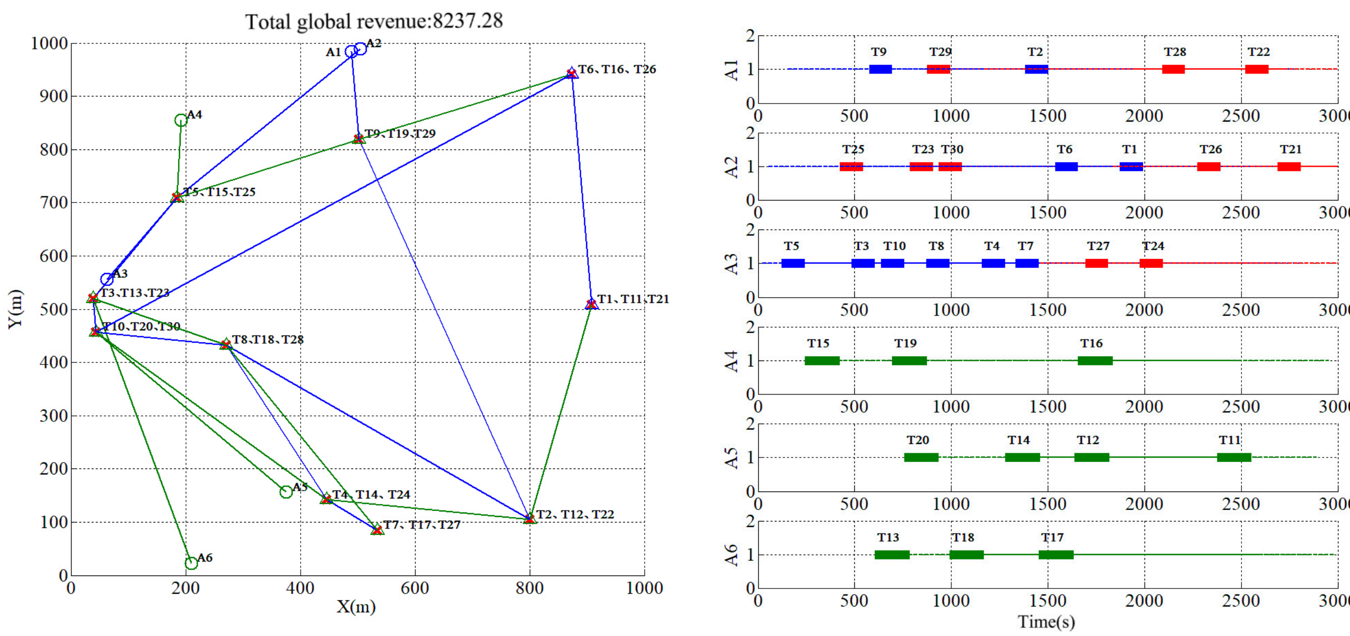

Figure 7. Schematic diagram of SWCBBA-PR task allocation result plane with task timing diagrams.

After task reassignment by the SWCBBA-PR algorithm, the task paths assigned to each AUV and the timing of the specific execution tasks are shown in Figure 7.

In Figure 7, it is evident that the heterogeneous AUVs are capable of fulfilling all the subtasks within the stipulated time, and no task conflicts occur among the AUVs during task execution. From the color-matching of the AUVs executing the tasks and the subtask points, it can be seen that the task allocation scheme satisfies the heterogeneous task execution capability constraints of the multi-AUV system. Specifically, light AUVs execute search and confirmation subtasks, while heavy AUVs execute mine-neutralizing subtasks. From the figure, we can also see that there is no duplicate assignment of tasks in the allocation result, and an AUV can only execute one task at a time, and a task is only executed by one AUV, which satisfies the collaboration constraints of the heterogeneous multi-AUV system, improves the system's collaborative operation capability, and optimizes the system's resource allocation. At the same time, the search subtasks, mine-neutralizing subtasks, and confirmation subtasks of the same suspicious task point meet the required task coupling constraints, i.e., task priority requirements and task timing requirements.

Subtasks have an assignment rate of 100%, and the suspicious task point resolution rate also reaches 100%. The total global gain is 8237.28, which is about 1.5 times the rate before reallocation. Therefore, the SWCBBA-PR algorithm can realize the heterogeneous AUV collaborative task allocation for searching new tasks in MCM mission tasks. It produces a feasible and conflict-free task allocation scheme that complies with multiple constraints.

4.2. New Task Simulation of Algorithms for Being Found at Different Time Locations

From the task scenario, new task points are discovered at different times and locations, indicating they were detected within the detection range during different search-subtask executions. To verify the performance and superiority of SWCBBA-PR when new tasks are discovered during different search-subtask executions, this section first simulates the performance under such discovery scenarios and then introduces SWCBBA-NR and SWCBBA-FR for comparison.

In order to verify the performance of SWCBBA-PR during the execution of different search subtasks, Table 4 shows the average task-assignment rate, global total gain, convergence time, and reallocation number for 100 Monte Carlo simulations under the conditions of $N_A = 6$, $N_t + n^* = 30$. Owing to page limitations, only the integer parts of the global total gain and convergence time are retained in Table 4.

Table 4. Performance under the discovered condition at different search-subtask executions.

Performance Indicators	**Search Subtasks in Progress When Discovering New Task Points**							
	T1	**T2**	**T4**	**T5**	**T6**	**T7**	**T8**	**T9**
Mandate distribution rate	100%	100%	100%	100%	100%	100%	100%	100%
Total global gain	8304	8145	8332	8073	8157	8107	8280	8621
Convergence time (s)	42	41	40	33	41	43	41	32
Number of redistributions	74	72	71	68	70	78	74	62

From Table 4, under different search-subtask execution conditions, the global total gain is generally stable at over 8100. The convergence time is generally stable at around 40, and the number of reallocations is generally stable at around 70. The main difference when executing different search subtasks is that the positions of new suspicious task points are randomly distributed within the AUV's detection range. This leads to varying navigation losses when executing subtasks for new task points, causing fluctuations in the overall global gain. The closer the distance, the smaller the decay of the subtask's initial gain over time and the lower the navigation loss, thus increasing the overall gain. Based on the SWCBBA-PR algorithm process, the convergence time is related to the number of reallocations and the introduction of the partial reset mechanism. From the table, it can be seen that the convergence time is slightly larger than SWCBBA-CR, which is due to the introduction of a partial reset mechanism to handle newly emerging task points, increasing computational complexity. The number of reallocations is basically consistent with the execution of the SWCBBA-CR algorithm, indicating that the introduction of a partial reset mechanism has almost no impact on the execution of the communication reassignment process, and the change in the number of reallocations is mainly related to the position of the new task point. However, regardless of which search subtask the new suspicious task point is discovered during execution, the task allocation rate can remain stable at 100%, and the task allocation scheme can meet the task coupling constraints of MCM mission tasks, achieving optimal resource allocation for multi AUV systems.

The advantage of SWCBBA-NR is that the convergence of the algorithm is almost unaffected by new tasks, and the algorithm will never consider reallocating existing task allocation schemes but only bid to insert new tasks into existing task packages. By effectively bidding only for new tasks and not allowing bidding for other tasks on its path, multi-AUV systems can achieve task reallocation very quickly. However, SWCBBA-NR has limited allocation flexibility, which leads to certain limitations on its global total gain. When a new task point is discovered, SWCBBA-FR needs to reset all previous task allocation plans to account for the new task. SWCBBA-FR provides the system with maximum flexibility when assigning new tasks, as this algorithm is completely unconstrained by previous task allocation schemes. Although this algorithm increases system collaboration, one drawback is that it no longer guarantees the convergence of the original task allocation problem, resulting in longer convergence times.

From Table 5, since SWCBBA-NR lacks a task reset mechanism, tasks in the previous task allocation scheme may occupy AUV resources. This leads to a poorer global total gain compared with the SWCBBA-PR algorithm. Due to the task reset of all tasks by SWCBBA-FR, its global total gain is consistent with the SWCBBA-PR algorithm. Compared with other algorithms, while satisfying the task priority and timing constraints in MCM mission tasks, SWCBBA-PR can arrange the optimal task timing for the subtask allocation of new task points. Thus, it can obtain the optimal average global total gain under different search-subtask execution conditions. That is, SWCBBA-PR can optimize the configuration of heterogeneous multi-AUV systems to generate better task allocation schemes.

Table 5. Average global total gain of algorithms under the condition of being discovered at different search-subtask executions.

Search Subtasks		**Arithmetic**	
	SWCBBA-PR	**SWCBBA-NR**	**SWCBBA-FR**
T1	8304.15	7523.49	8304.15
T2	8145. 83	7229.92	8145. 83
T4	8332.21	7529.39	8332.21
T5	8073.19	7123.29	8073.19
T6	8156.58	7242.30	8156.58
T7	8107.32	7209.24	8107.32
T8	8279.89	7301.28	8279.89
T9	8621.30	7618.92	8621.30

From Table 6, it can be seen that SWCBBA-FR needs to reset all tasks; that is, all task allocation steps need to be re-executed, and the convergence time is about twice that of the SWCBBA-PR algorithm. Because SWCBBA-NR does not perform task reset, its convergence time is about 5 s shorter than SWCBBA-PR's. However, the global total gain of the SWCBBA-NR algorithm is 10% worse than that of the SWCBBA-PR algorithm. In addition, under the condition where a new task is discovered during the execution of the search subtask T_9, the difference in convergence time between the SWCBBA-PR algorithm and the SWCBBA-NR algorithm is the largest, but their convergence times are both within the same range of magnitude, and the convergence time has only increased by 6.03 s, which meets the real-time requirements of the algorithm.

Table 6. The average convergence time (in seconds) of three algorithms under different search-subtask execution conditions.

Search Subtasks	Arithmetic		
	SWCBBA-PR	**SWCBBA-NR**	**SWCBBA-FR**
T1	41.67	36.89	81.88
T2	41.37	36.50	81.65
T4	40.39	34.76	79.75
T5	32.58	28.75	70.88
T6	40.60	34.91	79.94
T7	42.69	36.95	82.88
T8	41.49	36.51	81.53
T9	31.80	25.77	69.71

In summary, SWCBBA-PR is found to perform best under different search-subtask execution conditions and can produce more effective task allocation schemes. To address the new task allocation problem in the heterogeneous multi-AUV cooperative task allocation model for the scenario where new tasks emerge during MCM missions, SWCBBA-PR needs to introduce a partial reset mechanism. This slightly increases the computational complexity but enables obtaining a more optimal task allocation plan.

5. Conclusions

In this study, we considered the limitations of underwater acoustic communication. We successfully introduced the soft time window and partial reallocation mechanism into the CBBA algorithm, thereby creating the SWCBBA-PR algorithm. This algorithm enables collaborative task allocation for multiple heterogeneous AUVs when new suspicious task points emerge in the MCM mission scenario. This paper conducts simulation verification from two aspects:

(1) Verification of the algorithm's feasibility. A comparative analysis is carried out on the task allocation situations at four moments: the initial moment of task allocation, before the discovery of a new task point, after the discovery of a new task point, and after the completion of task reallocation. The results show that this algorithm can ensure full coverage of suspicious task points and a subtask allocation rate of 100%. The change in the global total gain of its allocation scheme conforms to objective laws.

(2) Comparative analysis of algorithm performance. In response to the situation where new task points are discovered during the execution of different search subtasks, 100 Monte Carlo simulations are conducted on three algorithms: SWCBBA-PR, SWCBBA-NR, and SWCBBA-FR. The results indicate that the total gain of the allocation scheme of SWCBBA-PR is consistent with that of SWCBBA-FR, while the convergence time is approximately half shorter than that of SWCBBA-FR. Although the convergence time of SWCBBA-PR is slightly higher than that of SWCBBA-NR, its global total gain is increased by more than 10%.

In conclusion, this algorithm not only meets the complex task time-sequence coupling constraints in the MCM task scenario but also fully utilizes the original allocation plan to efficiently re-allocate tasks when new suspicious task points appear. This algorithm has better optimization and convergence performance and is suitable for task allocation in the MCM mission scenario. Meanwhile, it is expected to be improved and expanded in other fields.

Although this study builds on the CBBA algorithm and has achieved some results in task allocation of heterogeneous multi-AUVs, the research has not fully considered various real-world factors. Therefore, significant follow-up research is still required, including the following:

(1) Collaborative path planning for heterogeneous multi-AUVs. This paper only studies the execution of mission tasks from the task-allocation aspect. The paths used in the decision-making process are merely point-to-point straight-line distances. How to select paths that meet the maneuverability requirements of the heterogeneous multi-AUV system is another pressing issue.
(2) Task allocation in a three-dimensional complex underwater environment. This study is conducted in a two-dimensional planar environment. However, the actual area for mission task execution is a complex three-dimensional underwater region. In this region, there are many complex and variable factors, such as ocean currents, tides, and marine organisms, which pose more complex challenges to AUVs in mission task allocation.
(3) Collision and obstacle avoidance among heterogeneous multi-AUV systems. This study assumes that all mission task execution areas are in the deep sea without considering the collisions between obstacles and AUVs in the system. With the increase in the number of AUVs in the task execution area, further research on collision and obstacle avoidance in the collaborative task allocation of heterogeneous multi-AUVs is needed.

Author Contributions: Conceptualization, J.L. and B.L.; methodology, J.L. and B.L.; software, B.L. and C.L. (Cong Lin); validation, C.L. (Caiyun Liu) and C.L. (Cong Lin); formal analysis, C.L. (Caiyun Liu); writing—original draft preparation, J.L., B.L. and C.L. (Cong Lin); writing—review and editing, J.L., B.L., C.L. (Caiyun Liu) and C.L. (Cong Lin); supervision, J.L. and C.L. (Caiyun Liu). All authors have read and agreed to the published version of the manuscript.

Funding: This research received no external funding.

Institutional Review Board Statement: Not applicable.

Informed Consent Statement: Not applicable.

Data Availability Statement: Dataset available on request from the authors.

Conflicts of Interest: The authors declare no conflicts of interest.

References

1. Li, J.; Zhang, K.; Xia, G. Multi-AUV cooperative task allocation based on improved contract network. In Proceedings of the 2017 IEEE International Conference on Mechatronics and Automation, Takamatus, Japan, 6–9 August 2017. [CrossRef]
2. Zhou, Z.; Shen, G.; Niu, W.; He, B.; Shen, Y. A task assignment strategy for multi-AUV collaborative hunting problem. In Proceedings of the OCEANS 2022, Hampton Roads, VA, USA, 17–20 October 2022. [CrossRef]
3. Guo, L. Research on Task Allocation Strategy for Heterogeneous Multi-AUV Systems Based on Auction Mechanism. Master's Thesis, Yanshan University, Qinhuangdao City, China, 7 June 2021.
4. Zhang, Z.; Wang, J.; Xu, D.; Meng, Y. Task allocation of multi-AUVs based on innovative auction algorithm. In Proceedings of the 2017 10th International Symposium on Computer Intelligence and Design, Hangzhou, China, 9–10 December 2017. [CrossRef]
5. Wang, Y.; Li, H.; Yao, Y. An adaptive distributed auction algorithm and its application to multi-AUV task assignment. *Sci. China Technol. Sci.* **2023**, *14*, 1235–1244. [CrossRef]

6. Choi, H.L.; Brunet, L.; How, J.P. Consensus-based decentralized auctions for robust task allocation. *IEEE Trans. Robot.* **2009**, *25*, 912–926. [CrossRef]
7. Johnson, L.; Ponda, S.; Choi, H.-L.; How, J. Improving the efficiency of a decentralized tasking algorithm for UAV teams with asynchronous communications. In Proceedings of the AIAA Guidance, Navigation, and Control Conference, Toronto, ON, Canada, 2–5 August 2010. [CrossRef]
8. Kim, K.S.; Kim, H.Y.; Choi, H.L. A bid-based grouping method for communication-efficient decentralized multi-UAV task allocation. *Int. J. Aeronaut. Space Sci.* **2020**, *21*, 290–302. [CrossRef]
9. Zhao, T.; Deng, H.; Gao, J.; Huang, J. Multi UAV dynamic target allocation based on network node clustering. *J. Syst. Simul.* **2023**, *35*, 695. [CrossRef]
10. LI, J.; Huang, W.; Wu, H.; Cai, Z.; Zhang, Y. OL-CBBA: An online task allocation algorithm under weak communication conditions. In Proceedings of the 2023 IEEE 29th International Conference on Parallel and Distributed Systems, Hainan, China, 17–21 December 2023. [CrossRef]
11. Binetti, G.; Naso, D.; Turchiano, B. Decentralized task allocation for surveillance systems with critical tasks. *Robot. Auton. Syst.* **2013**, *61*, 1653–1664. [CrossRef]
12. Fu, X.; Feng, P.; Li, B.; Gao, X. A two-layer task assignment algorithm for UAV swarm based on feature weight clustering. *Int. J. Aerosp. Eng.* **2019**, *2019*, 3504248. [CrossRef]
13. Ma, Y.; Liu, Y.; Yang, Y. Multi-UAV autonomous collaborative task assignment based on coherent swarm algorithm. *Unmanned Syst. Technol.* **2021**, *12*, 123–143. [CrossRef]
14. Tang, J.; Li, X.; Dai, J.; Cao, Y. Heterogeneous multi-intelligent body coalition task allocation under complex constraints. *Control. Theory Appl.* **2020**, *37*, 1232–1245. [CrossRef]
15. Qiu, X.; Zhu, P.; Hu, Y.; Zeng, Z.; Lu, H. Consensus-Based dynamic task allocation for multi-robot system considering payloads consumption. In Proceedings of the 2024 China Automation Congress, Qingdao, China, 1–3 November 2024. [CrossRef]
16. Zakaria, C.; Nabil, A.; Shashank, G.; Fabio, P.; Geert, D.C. Towards learning-based distributed task allocation approach for multi-robot system. In Proceedings of the 2024 10th International Conference on Automation, Robotics and Applications (ICARA), Athens, Greece, 22–24 February 2024. [CrossRef]
17. Gao, C.; Du, Y.; Bu, Y.; Liu, Y.; Yang, X. Multi-UAV distributed tasking based on sequentially extended consistent packet algorithm. *Control. Decis. Mak.* **2022**, *42*, 534–570. [CrossRef]
18. Buckman, N.; Choi, H.L.; How, J.P. Partial replanning for decentralized dynamic task allocation. In Proceedings of the AIAA Scitech 2019 Forum, San Diego, CA, USA, 7–11 January 2019. [CrossRef]
19. Li, X.; Tang, J.; Dai, J.; Bo, N. Dynamic Task Allocation for Heterogeneous Multi-agent Coalitions. *J. Northwestern Polytech. Univ.* **2020**, *38*, 1094–1104. [CrossRef]